URTeC: 2994

Artificial Intelligence for Production Optimization in Unconventional Reservoirs

Oscar Molina*, Camilo Mejia, Jerry Webb, and Rebecca Nye, Enovate Upstream

Abstract

This work presents two cases for the application of artificial intelligence (AI) techniques as complementary tools to classic physics-based modeling. On the one hand, we discuss the benefits from the implementation of an AI-assisted non-linear solver, especially designed for analytical simulation of multi-fractured horizontal wells, that led to obtaining fast simulation results, this way opening an avenue for the use of reservoir simulations for type-well analysis in unconventional reservoirs.

On the other hand, we introduce the application of AI for drilling, more specifically, optimization of the rate of penetration (ROP). In both cases, we used data from offset wells to better understand the characteristics of the target formation, pinpoint opportunities for ROP optimization, and identify key production drivers to determine their impact on short and long-term production. In this manner, we are able to generate physically meaningful production forecasts.

In this paper, we examine the results from the application of the proposed AI methods to a field case study for a type-well study in the Lower Eagle Ford formation. Analysis of results show the importance of accounting for static reservoir properties and completion properties to generate accurate production forecasts. Similarly, we observe that the introduction of artificial neural networks (ANN) as a means for ROP optimization, using offset wells data, allowed to generate optimized drilling schedules to be used for drilling infill wells in the area of interest.

Introduction

In recent times the shale oil & gas industry has been tremendously impacted by a number of factors which have led to a market volatility in recent years. Among these factors, steep production declines (Hughes, 2013), the lack of physics-based modeling of using decline curve analysis (DCA) methods in multi-fractured horizontal wells experiencing very long transient flow (Belyadi and Yuyi, 2015), and the uncertainty of determining estimated ultimate recovery (EUR) from unconventional reservoirs with such methods

(Wang, 2017). Altogether, these factors have whooshed away investors thus deepening the economic crisis on the shale industry (e.g. Cunningham, 2020; Elliot, 2019).

In addition to market volatility, the financial crisis induced by the current global pandemic of COVID-19 makes it challenging for most E&P companies to maintain the levels of production operations observed earlier this year, when oil price was poised to rebound. Consequently, long-term financial performance of shale oil and gas projects have also been compromised by this external factor (Ozili and Arun, 2020). From a micro-economics perspective, the unconventional oil and gas markets' lack of focus on the return of investment may be deemed as one of the main culprits for their current financial struggle. Operational efficiency in US unconventional reservoirs has reached higher levels compared with conventional reservoirs (Dickson, 2019). However, the steep decline in shale oil production remains as one of the key challenges to tackle in order to ensure financial stability, at least from the petroleum economics side.

Digital technologies with a focus on integrated digitalization across the upstream value chain and workflow automations are part of the steps forward for the industry (Lu et al., 2019). As a consequence, remote operations, digitalization, reservoir and production automation, plus a focus on the return of investment, are the main components driving the application of modern technologies like cloud-based computing, artificial intelligence, and automated workflows.

In this paper, we introduce the application of a cloud-based, AI-driven digital ecosystem for optimization in the upstream value chain. The central component of this digital ecosystem is the ability to reliably forecast production from type wells using physically meaningful parameters, such as static reservoir properties, completion properties, and, more importantly, production history from offset wells. Understanding production drivers from a target formation allows to properly determine the technical production limits from type wells, which delivers a more realistic production expectancy hence petroleum economics, without the need for physics-less DCA-based predictions. Two components of the workflow, namely production forecasting and ROP optimization, are implemented for a field case study in the Lower Eagle Ford. **Figure 1** illustrates the integrated production enhancement and optimization approach discussed herein.

Unlike typical reservoir engineering workflows based on DCA, our starting point was the assessment of the technical limits for well performance in the target reservoir. This was achieved by creating a physics-based type-well study, focused on using historical production data from offset wells in the same area and formation to extract static reservoir properties and stimulated rock volume (SRV) properties by means of history-matching a physics-based reservoir simulation tool with field observations.

Following this approach, we were able to identify key short and long-term production drivers and determine their impact on expected well productivity. More importantly, the use of calibrated (i.e., history-matched) reservoir models for creating the type well ensures that production forecasts generated with the type well are realistic and represent the physics of fluid flow in the target formation. Sensitivity analysis of well production to variation in calibrated properties yields the expected technical production limits of the area of interest. Production data is presented in a normalized fashion in this work.

Once the technical production limits and production drivers have been properly identified, other aspects of the upstream value chain can be optimized. For instance, if a type-well analysis suggests that static shale (tight) reservoir properties are the most impactful drivers at mid-to-late times, then drilling engineers should focus their optimization strategy on increasing ROP while reaching production sweet spots, i.e., streaks of high porosity and high permeability in the target reservoir. This way, while the workflow assumes average static reservoir properties, this is not the case for drilling optimization therefore a tailor-made geosteering program, paired up with an ROP-optimized schedule, is expected to deliver the best results from the operational and economical standpoints.

This paper is divided as follows: the first part discusses the collection of static reservoir properties in preparation for the construction of the type-well analysis. Rock and fluid properties and correlations, including pressure-dependent permeability to simulate geomechanics effects on production, are discussed in

this section. Next, we shift the focus to completions design where we examine the collection of typical completions design for wells in the region of interest and utilize the 2-D Perkins-Kern-Nordgren (PKN) fracture propagation model to determine average fracture dimensions for the fracturing fluids commonly used by the operator. Here, we considered a material-balance approach to estimate fracture dimensions assuming the same fracture geometry in all fractured stages.

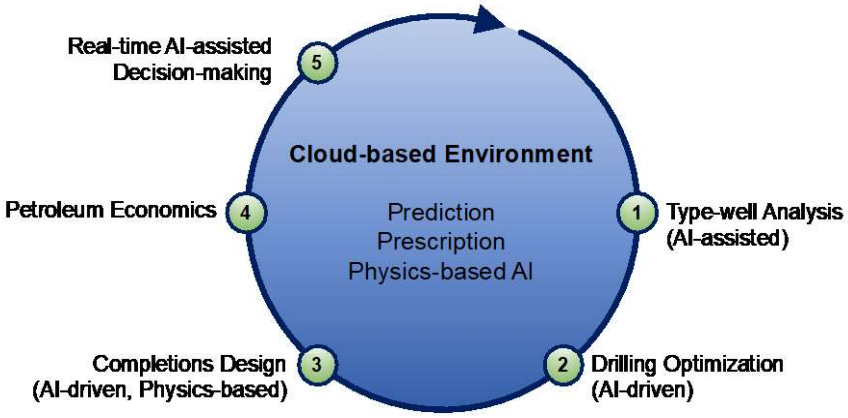

Figure 1. Integrated production enhancement and optimization workflow

After this section, we introduce the analytical multi-fractured horizontal well model used for reservoir simulations and examine the simulation workflow implemented in the present work, which includes the introduction of an AI-assisted convergence acceleration tool which also maintains the nonlinear solution process numerically stable. Later, we compare the history-matching results obtained for an offset well using the variable-rate and smoothly decaying bottomhole flowing pressure (BHFP) models. Calibrated reservoir and completion properties are then used to construct the type well and perform sensitivity studies to determine its technical production limits. Finally, we have a brief discussion about the application of AI methods, more specifically ANN, for ROP optimization, based on drilling data from several offset wells in the area.

Reservoir Characterization

The first and, arguably, the most important step towards production optimization within the cloud-based framework shown in **Figure 1** is the identification of the key production drivers in the target zone and understanding their influence in short and long-term production. These parameters may include static reservoir properties, reservoir fluid type and thermodynamic behavior, as well as completion design and efficiency. Because of the multi-variate nature associated with reservoir characterization, we aimed at reducing uncertainties, particularly for static reservoir properties, by virtue of cross-validating geological and petrophysical information and logs from offset wells, provided by the operating company, against publicly available data sources.

Reservoir Thickness. Static reservoir data from offset wells, in the area of interest, indicated an average pay thickness of 104 ft whereas an isopach map of the Eagle Ford shale shown in **Figure 2** (EIA, 2014) suggests that pay thickness varies between 75 and 150 ft across northwestern Karnes County. The exact location of the objective wells allowed us to narrow down this range and we concluded that a net pay thickness of 144 ft would be representative of the target zone in the lower Eagle Ford formation. Compliance effects were not considered in this study.

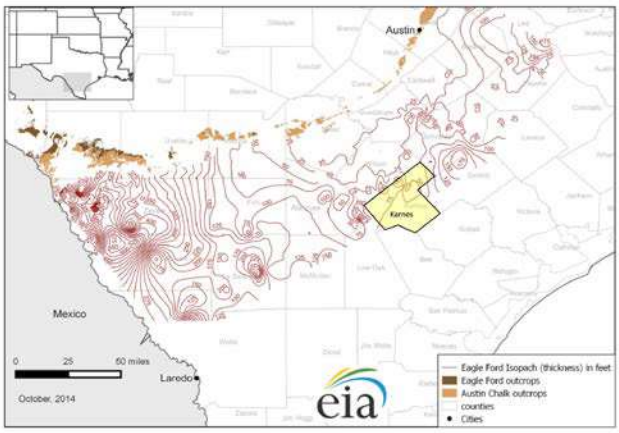

Figure 2. Thickness contour map of the Eagle Ford shale (EIA, 2014)

Matrix Porosity and Permeability. Determining porosity and permeability of the target formation was not as straightforward as pay thickness. E&P operator's knowledge on static reservoir properties of the Lower Eagle Ford in the Karnes County was principally obtained from petrophysical logs and porosity-permeability correlations. Nonetheless, the probabilistic nature of static reservoir properties was evident, therefore we were not able to assign specific values for them. Instead, we determined probable ranges within which typical values of porosity and permeability were observed to lie within. In consequence, we established that matrix porosity varies between 4% and 10% while matrix permeability ranges from 50 to 500 nd (1 nd = 1E-6 md), both at initial pore pressure conditions.

Initial Reservoir Pressure. Reservoir data from offset wells indicate that the region of interest in the Lower Eagle Ford is likely overpressured so that pore pressure gradient is significantly above the hydrostatic gradient. According to EIA (2014), pressure gradient in the Eagle Ford shale ranges from 0.5 to > 0.8 psi/ft. Given the depth of the target zone (~11200 ft), the initial pore pressure would lie between 5600 and 8900 psi. The pressure map shown in **Figure 3** (Gherabati et al., 2016) suggests that pore pressure in the Karnes County lies between 7500 and 8500 psi. To be consistent with all sources of information, we use 7500 psi as the initial pore pressure in this study.

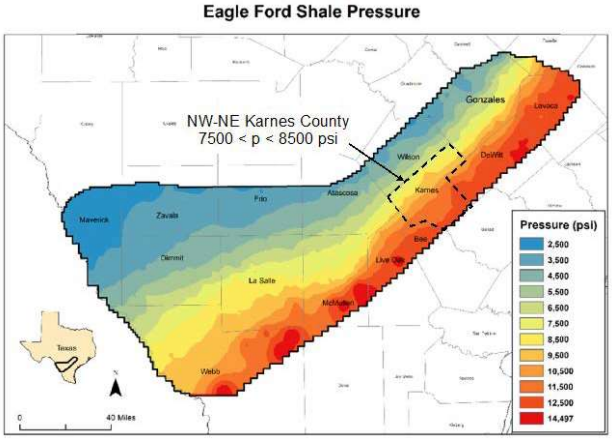

Figure 3. Average pore pressure in the Eagle Ford shale (Gherabati et al., 2016)

The fact that the reservoir section under study is over-pressured raises the need to accounting for the impact of large pressure drawdown on porosity and permeability. As such, we implemented the classic exponential-law model to model porosity as a function of pressure (Dake, 1983):

$$\phi = \phi_i e^{-c_r(p_i - p)} \quad (1)$$

where ϕ_i is porosity at initial pressure p_i [psi] and c_r [1/psi] rock compressibility. Though a value range for c_r for the Eagle Ford is not commonly found in the literature and/or would require specialized experimental testing, we use c_r = 5E-6 1/psi (e.g. Chaudary et al., 2011). A similar pressure-dependent permeability correlation was introduced into the reservoir model to incorporate geomechanics effects (Yilmaz and Nur, 1985):

$$k = k_i e^{-\gamma(p_i - p)} \quad (2)$$

where k_i is matrix permeability at initial pore pressure and γ [1/psi] permeability modulus. Similar to matrix rock compressibility, value ranges for γ are rather difficult to obtain without proper laboratory data of the matrix rock under study. However, data from the literature shows that 1E-4 $< \gamma <$ 5E-4 1/psi is a typical range for fractured rocks in major tight oil and gas basins across the US (Yao et al., 2015; Abass et al., 2009; Zhang et al., 2014). Therefore, we considered the case of low, moderate, and high geomechanics effects with γ = 1E-4, 2.5E-4 and 5E-4 1/psi, respectively.

Fluid Type and PVT Properties. We analyzed historic production data from offset wells in order to determine the type of reservoir fluid following the typical reservoir fluid characterization (McCain, 2017). In particular, this part of the study focuses on production data from the offset well OW-1. **Figure 4a** shows the cumulative oil and gas production from OW-1, normalized by their respective minimum monthly production. Notice that oil and gas production are almost proportional, which is typical of above-bubble-point-pressure producing conditions. The average producing gas-oil ratio (GOR) this well is 1421.67 scf/STB, which suggested we were dealing with a black-oil reservoir. This conclusion is supported by Gong (2013), as illustrated in **Figure 4b**.

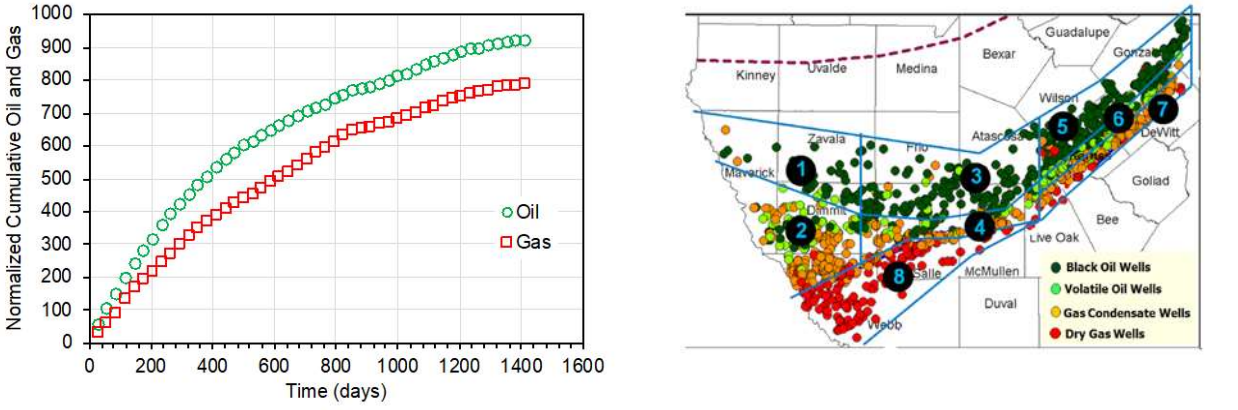

(a) Production history from well OW-1 **(b) GOR distribution in the Eagle Ford (Gong, 2013)**

Figure 4. Reservoir fluid characterization in the area of interest in Karnes County, south Texas

Because oil had been produced at above-bubble-point pressure conditions, we used the exponential law formulation to describe variations in oil formation volume factor with pressure (Dake, 1983):

$$B_o = B_{oi} e^{c_o(p_i - p)} \quad (3)$$

where B_{oi} [bbl/STB] is the oil formation volume factor at initial reservoir pressure p_i [psi]. Eq. (3) applies when p is equal or greater than the bubble-point pressure p_b [psi], which ranges from 2000 to 3800 psi in the area of interest (Gong, 2013; Yusuf, 2016; Gherabati et al., 2016). In addition, oil compressibility is assumed constant. Moreover, oil viscosity was assumed constant. **Table 1** summarizes the PVT properties used for production data analysis in this work.

Table 1. Typical Oil PVT Properties, Eagle Ford Shale (Karnes County)

Reservoir fluid type	Black oil
API gravity	42
Initial oil formation volume factor, c_o [rb/STB]	1.3513
Oil compressibility, c_o [1/psi]	4.8E-6
Initial oil viscosity, μ_o	0.549
Solution gas-oil ratio (GOR) [scf/STB]	1400

Contrary to produced gas volume, monthly oil production is rigorously booked therefore we focused our history-matching and model calibration efforts on oil production.

Well Completion Design

Similar to the workflow implemented to determine/estimate static reservoir properties and fluid properties, we collected information about completion design of offset wells in the area of interest and established a baseline for completion properties of the type well. While average stage spacing was found to be 200 ft, average fracture dimensions had to be either taken from the literature or estimated using fracture propagation models.

According to the E&P operator, the typical fracturing job size has an average pumping rate of 35 bpm for 45 minutes (per cluster), with a total of 5 clusters per stage. Additionally, the operator typically uses two different fluid formulations (Newtonian and Non-Newtonian). Moreover, we used petrophysical correlations to estimate Young's modulus and Poisson's ratio, $E = 6.38\text{E+6}$ psi and $\nu = 0.195$, respectively. We further undertake isotropic geomechanics properties and fracture-height-to-pay-height ratio r_p = 1.1, equivalent to 10% vertical fracture growth.

Based on this information, we implemented a nonlinear material balance for the PKN model (Smith and Montgomery, 2015) to estimated average fracture dimensions while considering 100% fracture growth efficiency; that is, we neglected stress shadowing and compressional and tectonic effects. Calculation results for fracture dimensions using the PKN model for a single-cluster stage are summarized in **Table 2**.

Despite petrophysical and geochemistry data from offset wells was readily available, the E&P operator decided to continue utilizing a geometric completion design. Therefore, we considered a geometric stage design for the type well. Thus, all fractured stages were assumed to have equal dimensions and completion characteristics, such as stimulation efficiency. Furthermore, although these results are compatible with other studies in the literature (e.g. Gong, 2013), detailed completion information was not immediately available for OW-1. Therefore, we reckoned that 400 ft fracture half-length was a conservative number for the type-well study, given that well spacing in future multi-well pads in the field of interest may become tighter than in legacy pads in the area.

Table 2. Fracturing Fluid Properties and Resulting Average Fracture Properties

Fracturing fluid type	Flow consistency index (K, cP-s^{n-1})	Flow behavior index (n)	Fracture half-length (ft)	Average fracture width (ft)
Newtonian	200	1	665.39	0.01632
Non-Newtonian	200	0.75	636.62	0.01841

Multi-fractured Horizontal Well Model

We used the five-region flow (FRF) model (Stalgorova and Mattar, 2013) as the reservoir model to history-match production data from OW-1, generate production forecasts for the type well, and create sensitivity studies to determine the impact of reservoir and completion properties on early and late-time production.

The FRF model was developed on the basis that fluid-flow from the matrix into the wellbore can be simplified as a combination of five different linear flows along with a choking skin damage due to flow convergence from the fracture into the wellbore (Stalgorova and Mattar, 2013; Brown et al., 2011). Fractured stages in the FRF are modeled as a composite system comprised of unstimulated rock (regions 2, 3, 4), stimulated rock (or reservoir) volume (Mayerhofer et al., 2010), and a planar fracture (region F), as shown by **Figure 6**.

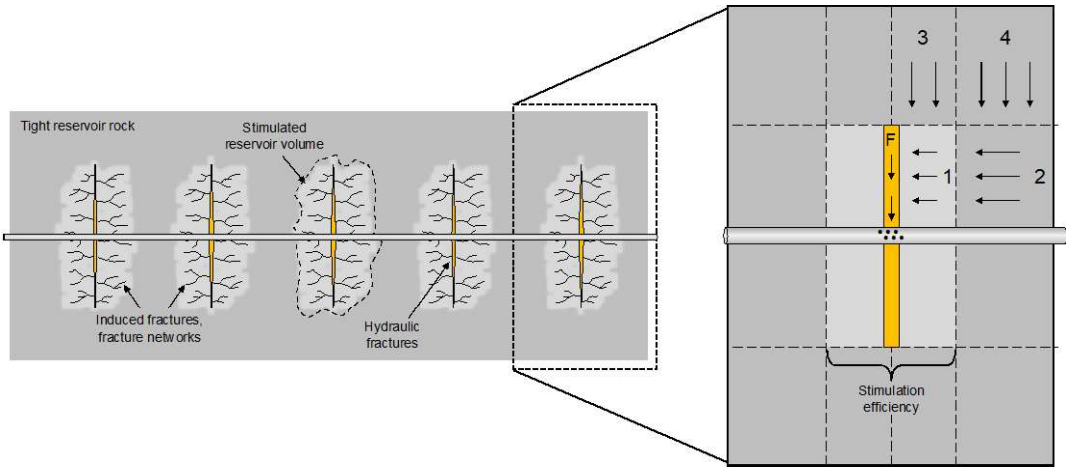

Figure 5. The five-region flow (FRF) model (Stagorova and Mattar, 2013)

The FRF model is an industry-standard model and, as such, it is commonly found in most commercial rate-transient analysis (RTA) software. Generally, two different versions are available: analytical and numerical. Despite its computational efficiency, the analytical FRF model has limited application because of the inherent restrictions of analytical solutions. Conversely, the numerical FRF model is very flexible and can override many of the assumptions of the analytical model, such as symmetric domain, constant rock properties, equal fractured stages. However, it is more computationally expensive henceforth, depending on the scope of the project, running recurrent numerical simulations may be restrictive.

For this study, we used Enovate Upstream's proprietary analytical version of the FRF model code-named ADA FALCON. This software was developed based on the original FRF model; however, it accounts for pressure-dependent rock and fluid properties without the need for using pseudo-functions to linearize the fluid-flow model. Instead, ADA FALCON includes a fast-nonlinear solver (FNS) (Molina, 2019) powered by a proprietary AI technology to accelerate convergence rates while ensuing numerical stability.

In this manner, we were able to obtain simulation results within seconds, even when we accounted for geomechanics effects acting on one or various regions, which is widely recognized as a factor that slows down numerical simulation times significantly due to the requirement of fine meshes and small timesteps.

Figure 6 illustrates the reservoir simulation workflow implemented in this work. The reservoir engineering study started with the analysis of production data from well OW-1 as well as static reservoir and completions properties in the area of study. Rock and fluid correlations were part of this initial stage. This information was fed into the analytical reservoir simulation model whose equations were solved by Enovate's proprietary fast nonlinear solver. The process was repeated until a satisfactory match was found. At this point, calibrated reservoir and completion properties were used to construct the type well model and physics-based probabilistic production forecasts are generated using the same reservoir simulator. Note that production drivers are identified as a result from the probabilistic (or sensitivity) analysis.

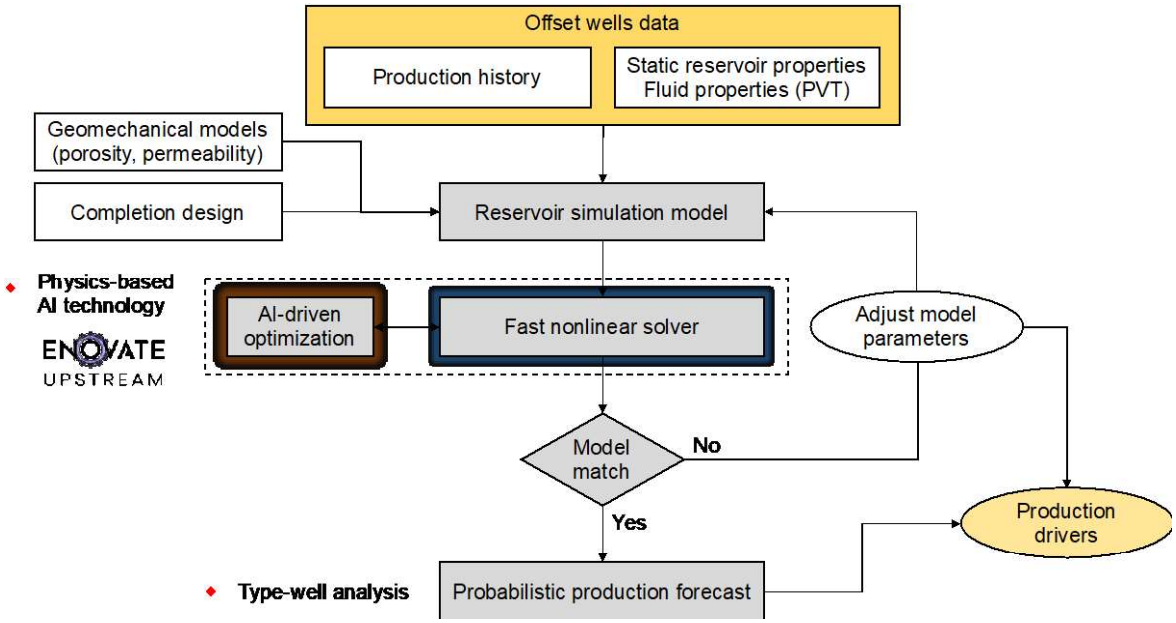

Figure 6. The five-region flow (FRF) model (Stagorova and Mattar, 2013)

Reservoir Model Validation

We considered two approaches for the reservoir model calibration process: variable-rate and smoothly decaying BHFP conditions (Fuentes-Cruz and Valko, 2015). Both models utilized actual production data from well OW-1. The calibration process was successfully achieved through fine-tuning reservoir properties and completion properties until a satisfactory match was found. **Figure 7** shows the history-matching results for the production history of well OW-1. **Figure 7a** compares analytical modeling results against actual production rates and cumulative production history. As it can be seen in this plot, the analytical model accurately captures production behavior up to the last data entry, which is ~4 years.

It is worthwhile to mention that bottomhole pressure data was not available for this study. Thus, to ensure the accuracy of the calibration process, we carried out variable-rate simulations, using production data as inputs, to generate the expected pressure response for a given model. Then, we used this synthetic pressure response to generate the rate and cumulative production response. This iterative process was performed until we found a satisfactory match between the model and production history. For simplicity, we simply refer herein to the whole process as variable-rate model calibration. With respect to the BHFP used

to generate the production forecast, we held the last synthetic flowing pressure constant. Relevant calibrated reservoir model properties are summarized in **Table 3**. We considered fully stimulated fractured stages (i.e. 100% stimulation efficiency) for this analysis and geomechanics effects were neglected. Note that the calibrated fracture half-length is in close agreement with those values estimated by the PKN model (Table 2).

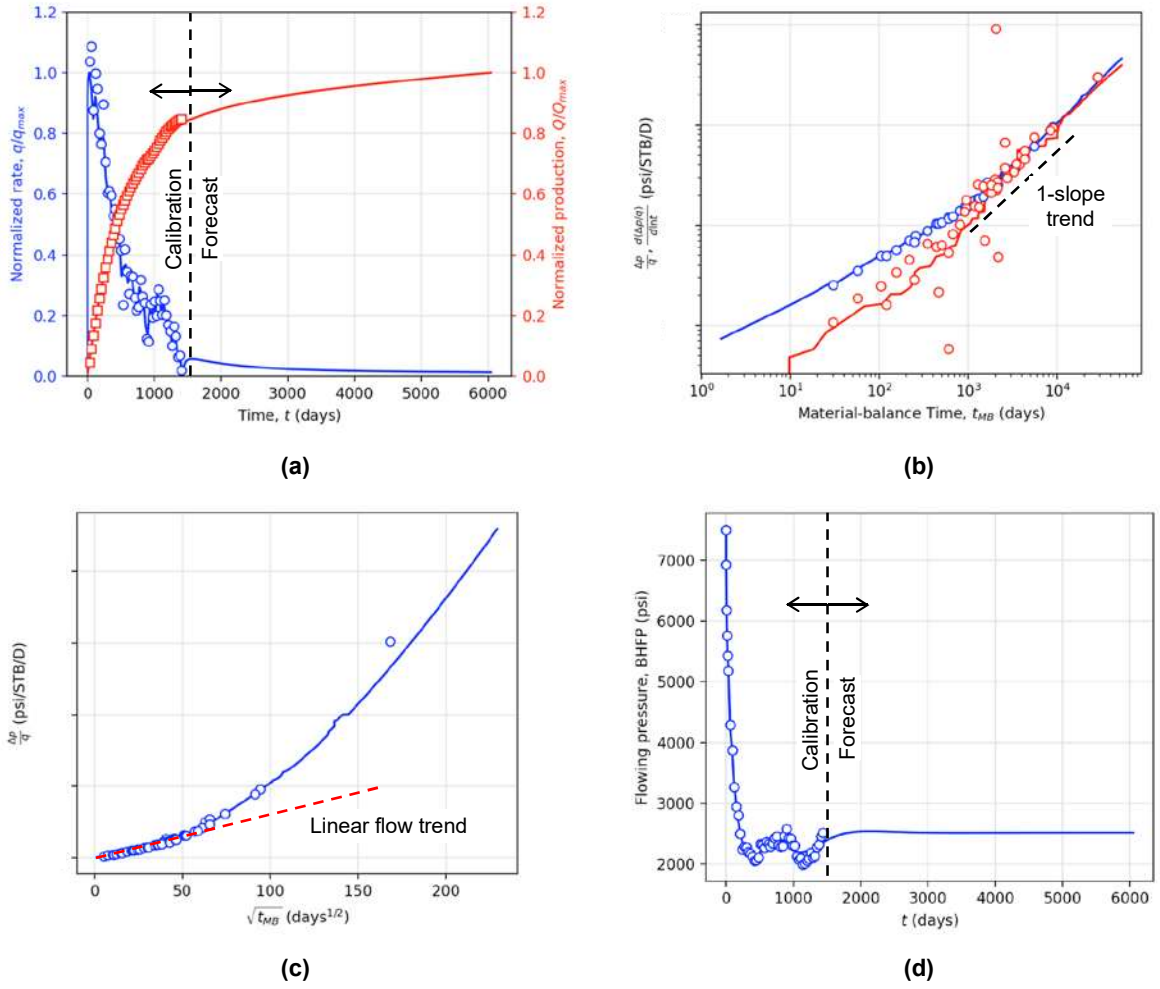

Figure 7. Model calibration for well OW-1 with variable-rate conditions (normalized production data are shown as symbols)

Table 3. Calibrated Reservoir Model Properties for Well OW-1

Reservoir pressure	7500 psia
Formation thickness	144 ft
Matrix porosity	8%
Matrix permeability	200 nd
Fracture half-length	660 ft
Fracture conductivity	200 md-ft
SRV permeability	850 nd
Bubble-point pressure	2000 psia

Daily rates and cumulative production for $t > 1450$ days, shown in **Figure 7a**, were generated by the reservoir model. Simulation results allowed us to conclude that OW-1 is positioned as one of the best performers in the area of study. According to **Figure 7b**, OW-1 is likely undergoing apparent boundary-dominated flow, that is, transitional flow from the SRV into the matrix. Notice the distinctive unit-slope trend exhibited by the rate-normalized pressure and its log-derivative. Therefore, one should expect that matrix properties would dominate well productivity during this stage of its productive life. Realize that this type of conclusions cannot be drawn by virtue of DCA methods.

Likewise, the specialized square-root material-balance time plot in **Figure 7c** indicates that transient linear SRV flow effects are relatively long-lived, compared to actual normalized production data. Note that most of the data lies within the linear trend within 0 and 50 days$^{1/2}$ (square-root material-balance time).

Similarly, we found a good match between observed field data and the analytical model for the case of smoothly decaying BHFP, as illustrated by the collage in **Figure 8**. For this scenario we utilized a stabilized exponential function for BHFP which starts at initial pressure and drops exponentially to the designated terminal BHFP (Fuentes-Cruz and Valko, 2015), which was set to 2200 psi. Furthemore, we chose the stabilization time to be 1 year. Reservoir and completion properties for this reservoir model were taken from those calibrated with the variable-rate model. Recognize that the difference between approaches is minimal thus confirming that the calibrated properties are physically sound.

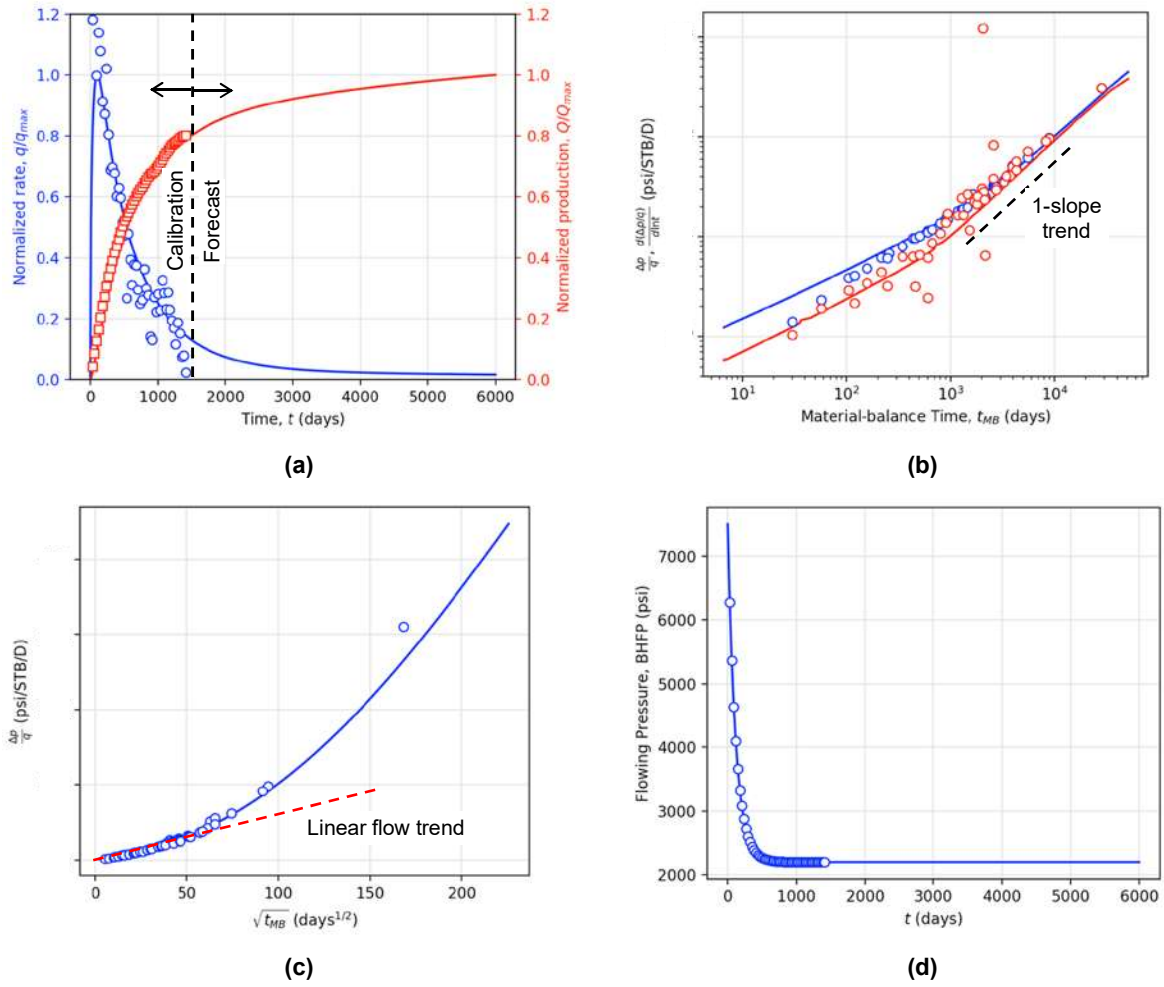

Figure 8. Model calibration for well OW-1 with an equivalent smoothly decaying BHFP

From the analysis of results in this section, we conclude that the five-region model, paired up with the fast nonlinear solver from ADA FALCON, is a powerful tool that supersedes DCA-type methods and enables reservoir engineers to get a broader picture of the physics and the influence of static and dynamic reservoir properties on model calibration and production forecast, as discussed in the next section. Moreover, note that reservoir and completion can be characterized with the help of calibrated models for use in type-well studies; this is not, by any means, achievable with DCA methods, at least for unconventional reservoirs.

The Need for Probabilistic Analysis

Reservoir engineers typically rely on forward and inverse reservoir modeling to calibrate reservoir properties of interest, useful for both diagnostics and production forecast (Oliver et al., 2008). On the one hand, forward models typically consider the reservoir model to be fully determined a priori, such that transient pressure and/or rate response is the outcome of the simulation process. On the other hand, transient pressure and/or rate response are typically known a priori in inverse models; however, the reservoir model and associated properties are initially unknown (Spivey and Lee, 2013).

In general, inverse models suffer from the problem of non-uniqueness (Spivey and Lee, 2013). In essence, this issue is related to the fact that several, if not many, reservoir models can reproduce the same expected response, in this case well production history. Due to this problem, inverse reservoir modeling typically involves the interaction of staff from various disciplines including geology and geophysics, engineering, and operations, with the final goal to gather as much data as possible in order to reduce uncertainties related to static and/or dynamics reservoir properties and completions characteristics.

Figure 9 illustrates an example of non-unique solutions for well OW-1. Realize that three different reservoir models—Model 1: base case (calibrated model); Model 2: low matrix permeability; Model 3: high SRV permeability—gave very similar decline rates and cumulative production curves. Nevertheless, production forecast curves depart from one another shortly after the last historical data entry. Thus, we found that it is more physically sound to define EUR as a range rather than a fixed value. Since most static reservoir properties are inherently probabilistic, due to anisotropy and heterogeneity, and, in other occasions, due to drilling out of zone, this type of analysis seemed prevalent for this study.

Despite the minimal variability in normalized EUR observed in Figure 9 (± 5%), Markov-Chain Monte Carlo simulations are needed to get a better picture of this variability (Sureshjani et al., 2020). This type of analysis is part of the future plan for this work. We instead ran a sensitivity study in the next section.

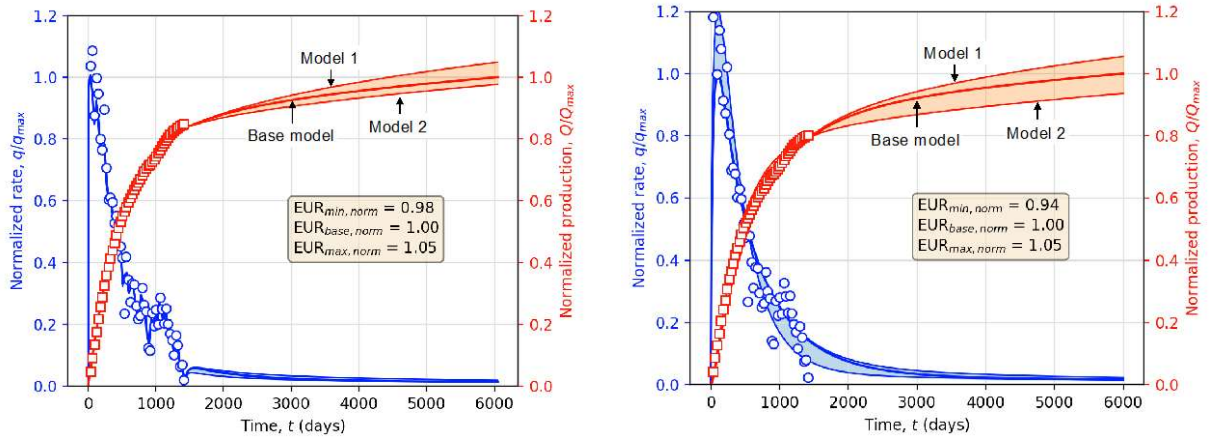

Figure 9. Probabilistic production forecasting and EUR estimation for well OW-1

Type-Well Analysis

Type-well production forecasts are derived for smoothly decaying BHFP conditions. Average daily oil rates and cumulative production are given at standard conditions using downhole conditions as the reference state. Since we used BHFP instead of wellhead flowing pressure as the pressure of choice for the reservoir model, the oil formation volume factor should take care of downhole-to-surface conditions as oil production takes place at above-bubble-point pressure conditions. Moreover, the requirement of a constant BHFP generally requires that an artificial lift system (ALS) be in place and running to sustain constant pressure flowing conditions; however, design and selection of ALS is out of the scope of this study.

In the following sensitivity analyses, we used the calibrated reservoir model as the based case and then varied several properties of the model in order to obtain different decline rates and cumulative production curves which allowed us to generate production envelopes, as discussed in the previous section. More specifically, we discuss the early and late-time impact of such variability in reservoir and completion properties. Decline rates and cumulative productions are normalized by the highest value obtained from the reservoir simulation model for the base line model (i.e. calibrated model).

Impact of Matrix Properties. The impact of matrix porosity and permeability on productivity of the type well is illustrated by the normalized rate and normalized cumulative envelopes in **Figures 10a** and **10b**, respectively. Notice that both reservoir properties would can impact late-time cumulative production hence EUR of the type well. In particular, notice that underestimating porosity would diminish EUR by 5%, as shown in Figure 10a; however, a slight increase in matrix porosity can lead to a 22% overestimation of EUR. The impact of matrix permeability, although noticeable at late times, is not as severe as that of porosity, even for one order-of-magnitude variation in this property.

From Figure 10b, we can conclude that permeability alone can induce a ±5% variability in EUR estimations. More importantly, be aware that none of these conclusions could be drawn by focusing on the decline rate curves alone. Finally, recognize that the impact of matrix properties on well performance appears at late production times, which is consistent with the physics of fluid flow in tight reservoirs.

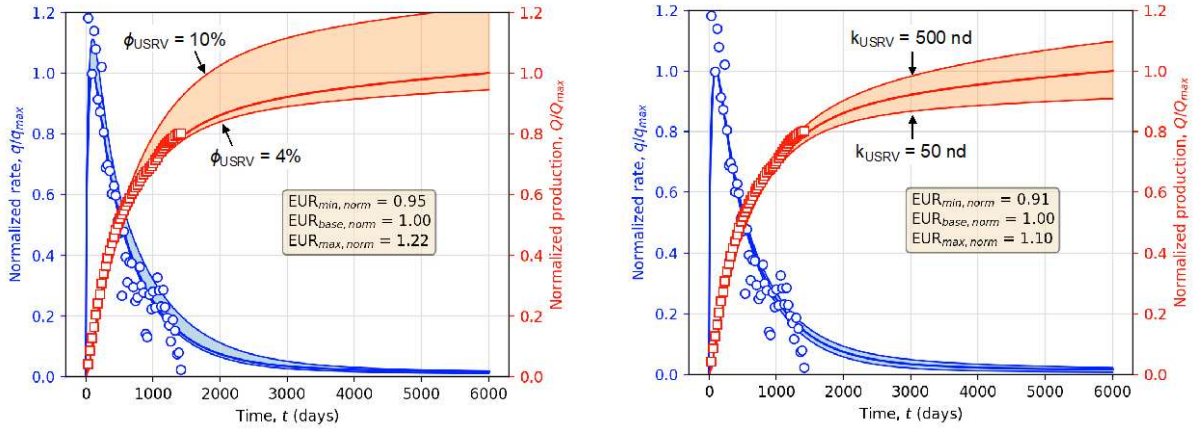

Figure 10. Impact of matrix properties on type-well performance: (a) porosity and (b) permeability

Impact of Completion Properties. In this analysis we consider the impact of the stimulation efficiency (how much of the fractured stage was effectively stimulated) and fracture conductivity. Be reminded that we considered 100% stimulation efficiency for the base line case. **Figure 11a** presents the effect of lower

stimulation efficiency in the type well. One thing one should notice almost instantly from this figure is that stimulation efficiency can impact early-time production thus hurting project economics and return on investment. Evidently, the choice of 100% efficiency for the base line model seems appropriate; however, it raises the question whether this assumption makes sense. As explained earlier, we concluded, based on both production data simulation results, that well OW-1 is an excellent performer in the area under study, therefore it is physically sound that this well may exhibit ~100% stimulation efficiency.

With respect to fracture conductivity, we concluded from **Figure 11b** that conductivities beyond 200 md would deliver the same performance compared to high-conductivity fractures. Once again, it makes sense that the calibrated model yielded a moderate fracture conductivity (200 md-ft) given that well OW-1 enjoys of high production performance compared to other offset wells in the area. Yet, notice that, if that was not the case, low fracture conductivity would have posed a detrimental impact on early-time production, thus having potentially jeopardize return on investment and financial projection for this well. This effect can be confirmed by the relatively high variability in the decline rate envelop at relatively early times.

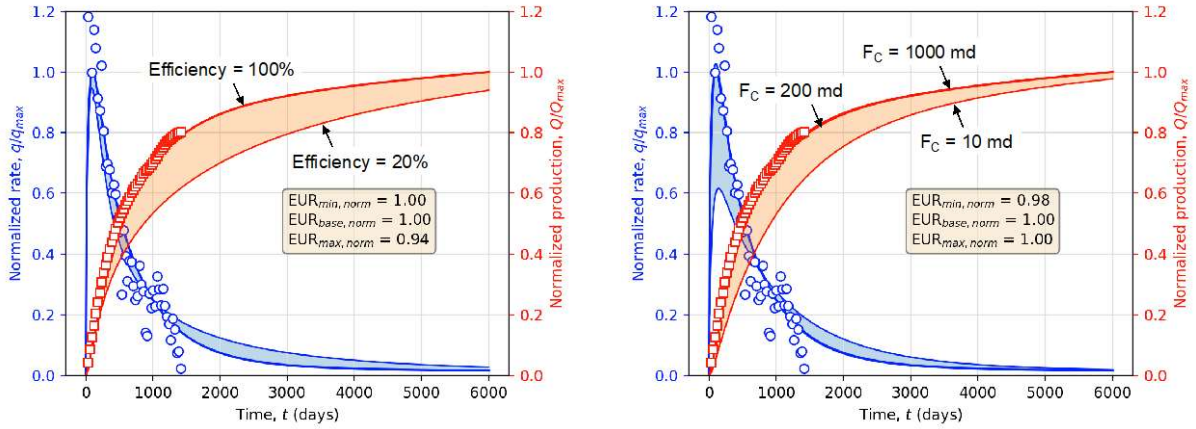

Figure 11. Impact of completion properties: (a) stimulation efficiency and (b) fracture conductivity

Impact of SRV Properties. The impact of SRV porosity and permeability on well productivity are shown in **Figure 12a** and **12b**, respectively. To begin with, recognize that the effect of SRV porosity on production appears to be more severe than that of matrix permeability (Figure 10a). For the lower-bound case, we assigned both matrix and SRV the same porosity, otherwise it would be challenging to defend SRV permeability being lower than matrix porosity. In this case, the combined impact of low porosity values on well productivity could surface at mid-to-late times (> 1 year of production) and its impact could reduce EUR estimation by 22%. Contrariwise, the upper-bound case, which considers matrix porosity and SRV porosity to be 8% and 12%, respectively, would deliver a production overestimation of 39% with respect to the base line case. In conclusion, similar to matrix porosity, incorrect estimation of SRV porosity can potentially lead to a sensible variability in EUR calculation, from 22% underestimation all the way to 39% overestimation.

Regarding SRV permeability, Figure 11b shows that this parameter influences early-to-mid-time production. This is a logical conclusion given that most of the production from multi-fractured horizontal wells comes from the stimulated rock volume, as indicated by the unit-slope trend exhibited by both production data and simulation results in Figure 7b and 8b, as well as the linear trend observed in Figure 7c and 8c. Interestingly, it appears that, regardless of SRV permeability, EUR estimation should not be as largely impacted by this parameters as it is by matrix and/or SRV porosity. This is due to the fact that SRV

permeability only controls the speed at which oil is produced from the well; the ultimate amount is dictated by the pore volumes of fluids that are able to escape from the reservoir into the wellbore, and this quantity is directly controlled by porosity. Nonetheless, early-to-mid-time reservoir economics may be either favored or adversely affected by SRV permeability, particularly rate of return and similar economics metrics.

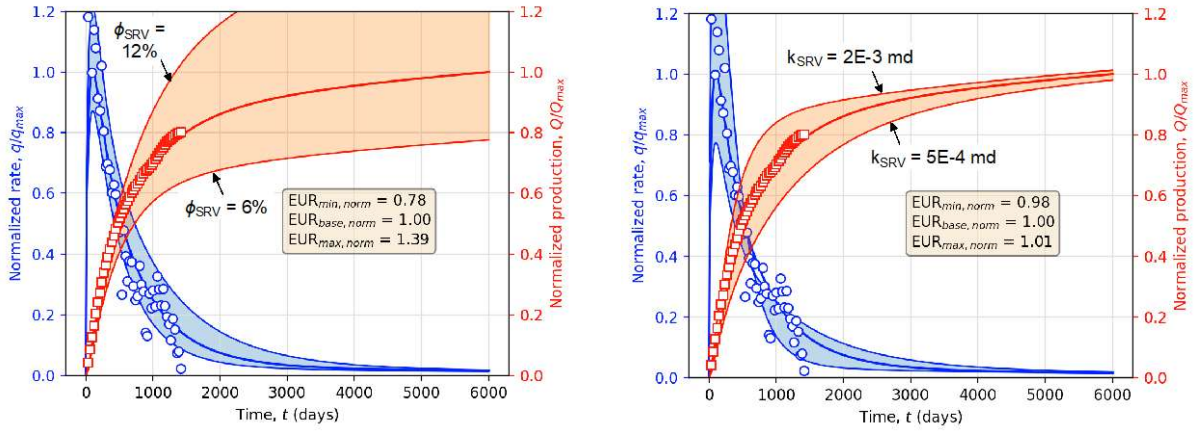

Figure 11 – Effect of (a) geomechanics and (b) hydraulic fracture conductivity on type-well performance

Impact of Geomechanics. At the beginning of the paper we emphasized on the formation being overpressured and presumed that geomechanics would play a major role in productivity from wells in the formation of interest. However, as explained in the reservoir model validation section, geomechanics effects were neglected, i.e. permeability was assumed constant, yet we were able to accurately history-match production history from well OW-1. Here, we considered that hydraulic fracture conductivity and SRV permeability are pressure-dependent and follow the exponential law model in Eq. (2). Furthermore, given that the SRV is mostly composed of unpropped fracture networks (Mayerhofer et al., 2010) that would tend to close faster than propped fractures (Zhang et al., 2014; Yao et al., 2016), we assigned permeability modulus of the SRV to be twice as much as that of the hydraulic fracture (i.e. $\gamma_1 = 2\gamma_f$).

The fact that the SRV and hydraulic fracture have distinct permeability moduli would make the application of the FRF model very difficult for analytical models. Nonetheless, this was not an issue for this study, because the nonlinear solver from ADA FALCON admits the use of distinct pressure-dependent correlations for permeability for the various regions of the FRF model, even if the correlations themselves are different. For instance, ADA FALCON allowed us to test different correlations for the hydraulic fracture than for the SRV, and simulation results were delivered without major issues. This demonstrates the power of the AI component within the solver that allows to run very complex simulations while accerelating convergence rates and maintaining the numerical stability of the solution.

Figure 12 shows that the effect of geomechanics was indeed absent from well OW-1. Note that the actual decline rate and cumulative production curves are located outside of the geomechanics envelopes. In any case, we can conclude that geomechanics has a tremendous impact throughout the productive life of the well, even from early-to-mid times, leading to a 6% (for moderate pressure dependency) to 20% (for strong pressure dependency) reduction in EUR due to SRV permeability being destroyed with pressure decline.

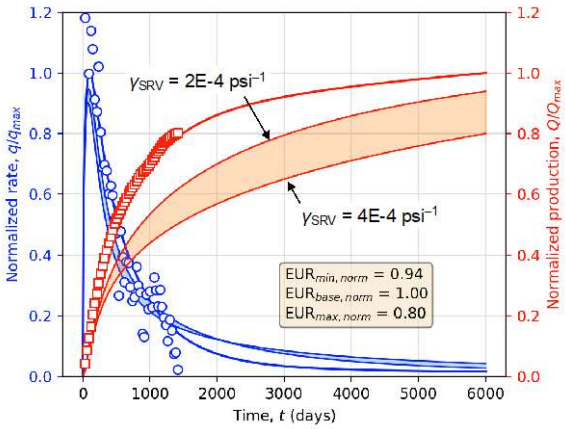

Figure 12 – Impact of geomechanics on performance of the type-well

Artificial Intelligence (AI) for Drilling Optimization

Once the drivers for reservoir productivity are identified from the physics-based AI model, the planning phase of new wells are improved by targeting specific, well defined prediction targets in real time. In this case study the AI model is trained from offset well data and the outcome from production module.

The real-time prediction capability is built by the integration of several machine learning models that constrain and guide the wellbore trajectory and drilling parameters in real time. Two specific targets for the drilling phase are to achieve the optimization of rate of penetration and the automated wellbore trajectory positioning in the areas of the reservoir that lead to greater completions efficiencies and therefore higher reservoir productivity.

Optimizing the Rate of Penetration. A successful AI driven automation is always a model that is trained for the specific challenge and with the assessment from the drilling expertise or domain knowledge. Several factors are considered to develop a comprehensive model prediction to determine optimal rate of penetration (the output) by use of drilling parameters (input).

In this case study, optimal ROP is defined as any ROP achieving above-average performance from the historical data set collected. One must ensure the data collected includes only the best performing wells drilled so the average acts as the datum for which any ROP achieved above represents improved performance. Establishing an average also ensures adequate data is represented above and below the performance KPI so the model can be adequately trained with enough data to achieve good accuracy with limited number of wells required.

Data Preparation and Model Prediction. Data preparation started with establishing a sorting criterion that ensured an "apples to apples" comparison when analyzing the data through the modeling process. Such information to establish this backdrop included:

- Rig equipment limitations (torque, rpm, pump pressure)
- Mud program (MW & PV)
- Well type and directional requirements (drag effect)
- Formation characteristics (US, elasticity, chemical composition, minerology)
- Bit information (type, material, cutters).

In addition, we determined that the data should also be free of incidents which may have occurred related to any torque, drag, vibration, or violation of hydraulic pressure in the wellbore. This ensured the end-result parameter suggestion is free of any data that may resulted in a violation of a safe drilling envelope.

Once the data was sorted, we cut-out any sliding intervals so only drilling ROP is examined without introducing any bias into the dataset (**Figure 13a**). Sliding can contaminate the results simply by the goal of sliding being different than that of drilling – i.e. sliding leans toward directional control vs. that of achieving higher ROP which is the goal when drilling. Erroneous data points (sensor noise, bad measurements) were also removed wherever deemed necessary and signal smoothing was applied on the raw data in order to filter out potential data outliers, as shown by **Figure 13b**.

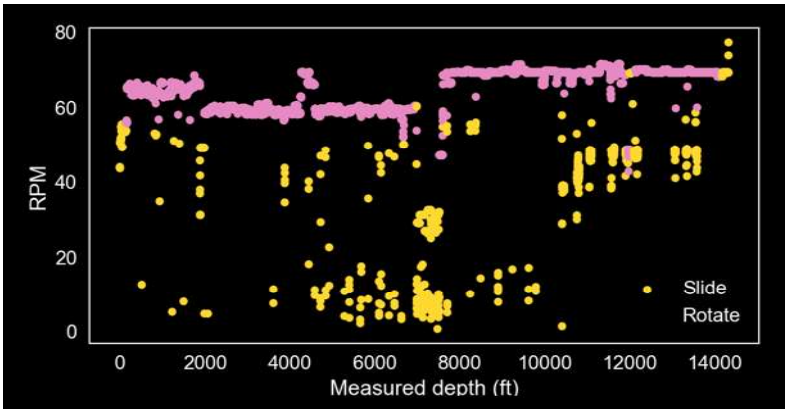

(a)

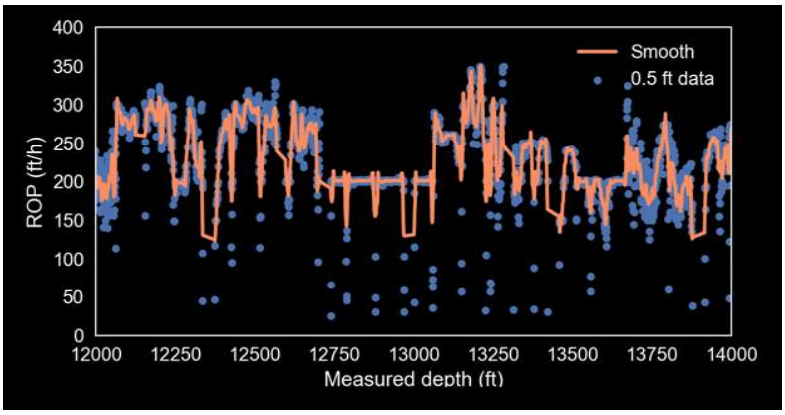

(b)

Figure 13 – ROP filtering and smoothing process

Once the data set was ready, we established what factors had a direct effect on ROP (at the bit face). This step will setup the inputs toward the model prediction. Factors include:

- Drilling parameters
- Bit information
- Motor configuration (if applicable)
- Cumulative tortuosity

As illustrated by **Figure 14**, the variables extracted from these factors are then feature-ranked by random forest to determine which have the largest effect on ROP. The process allows the user to choose as many variables as desired and observed their ultimate effect on ROP. In this study, we determined a set of 7 variables that had the largest impact on ROP on all the offset wells used for this analysis.

Once the variable ranking was completed, we moved into the modeling phase by virtue of the implementation of an artificial neural network (ANN), based on a classification problem. Basically, what we intended to do was to classify ROP data, depending on whether their value was above or below a certain threshold, such that Class 1 data complies with ROP > ROP_{avg} whereas Class 0 falls into the range ROP < ROP_{avg} (**Figure 15**). An example of the execution of the classification algorithm is presented in **Figure 16**.

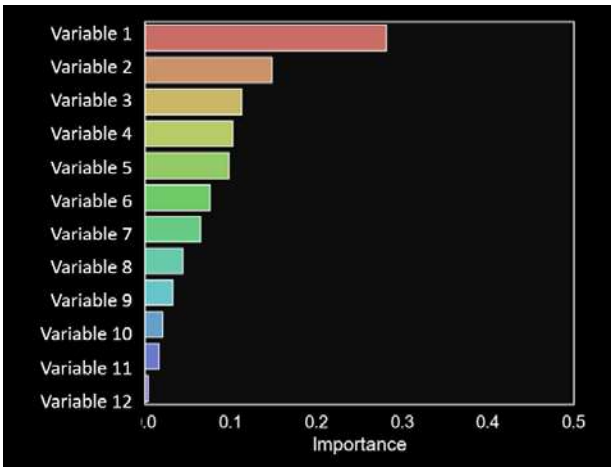

Figure 14 – Ranking process using random forest

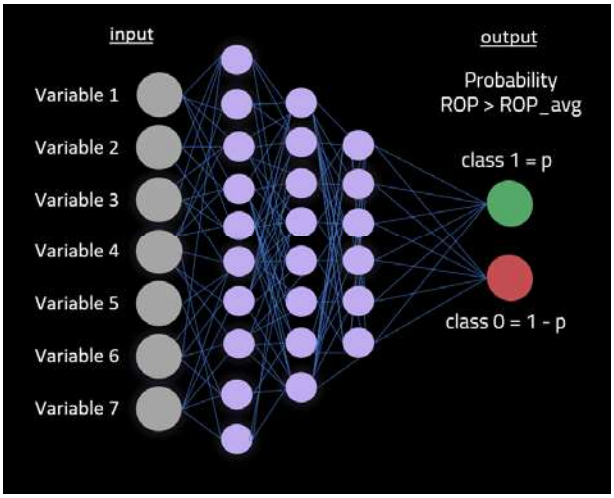

Figure 15 – Neutral Network modeling process

Based on the chosen set of variables which has the greatest impact on ROP, as confirmed from data evaluation, we performed the AI-based modeling for each formation drilled, to include any cases where motor and/or bit characteristics would have occurred. The conclusive results yield that, on average, using the proposed AI procedure, high accuracy for ROP prediction was achieved, which was in the order of 95%.

The next step, and one that poses more challenge, is to convert the variables (inputs) used in the model into something practical that drilling engineers and operations staff can use, both in the office and field, by way of common drilling parameters monitored on the rig floor as well as remotely, while also allowing an acceptable minimum and maximum threshold per parameter to account for any deviation that may occur during the drilling process (ex: flowrate reduction due to mud pump repair).

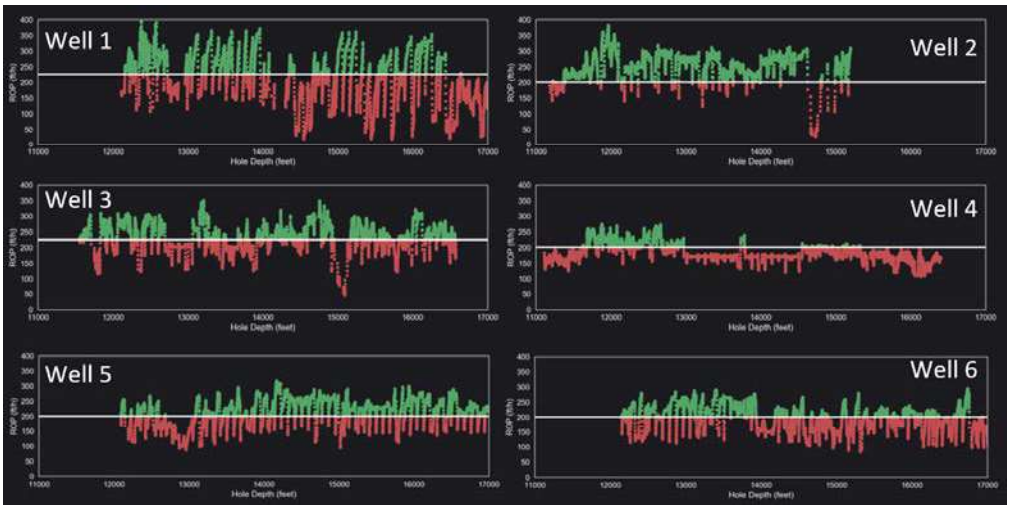

Figure 16. ROP datum from offset well data set

In the light of ROP optimization by virtue of AI, real-time management of the variables impacting ROP the most requires the simultaneous interaction of several, if not all, of these parameters. The simplest case was the scenario where ROP depends on only one of these parameters. In this case, a 1-D variation of ROP with respect to this parameter would result from the analysis, as shown in the first enclosed schematic on **Figure 17**. Note that all parameters would produce a similar plot, thus the viability of using a single parameter for optimization purposes may not be as straightforward nor physically meaningful.

The second case we developed relates to the mutual interaction between two parameters. This study yielded a 2-D heat map which gives a region within which the highest ROP would be seen, as shown in the second enclosed schematic on Figure 18. Although this was a significant improvement over the 1-D variation approach, still we got different trends and heat maps for different combinations of these properties.

Finally, we run a 3-D variation model to capture the drilling parameter 'cloud which yielded the optimal ROP setting at any given depth and formation in the target well. It is important to recognize that moving from 1-D variation to 3-D increases the accuracy of the ROP prediction; however, the complexity of the prediction model increased substantially as more variables were compared in the same volume.

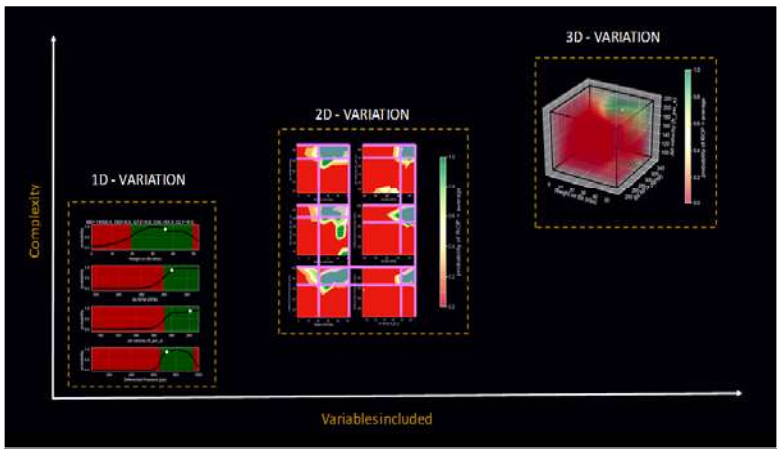

Figure 16. 3-D view of the ROP optimization process

In the end, we evaluated the simultaneous action of the 7 variables for ROP optimization. To do so, we relied on a cloud-based server to carry out the simulations with parallel computing and multi-threading technologies. As a matter of fact, we observed a substantial speed-up of the machine learning process after implementing multi-processing and multi-threading tools, in a way that we believe feasible to execute this type of optimization analysis with AI and machine learning while drilling; that is, near real-time drilling optimization.

In practicality, the validation and test of results showed a decline in the accuracy by up to 20% when testing the model with offset wells we solely used for testing, not training, purposes (**Figure 18**). Yet, 80% accuracy means that 80% of the time that the drilling crew follows the recommendation given by the AI model and parameter schedules are followed, the optimal ROP window will be achieved. More importantly, as mentioned earlier, following automated drilling parameters in real time, delivered via web-based visualization, will enable cross-platform drilling optimization on a single cloud-based ecosystem. In this manner, field personnel, service companies related to the wells under analysis, geoscience and engineering teams, and E&P management can all participate in the same process and delineate better practices for AI-based optimization and real-life field operations.

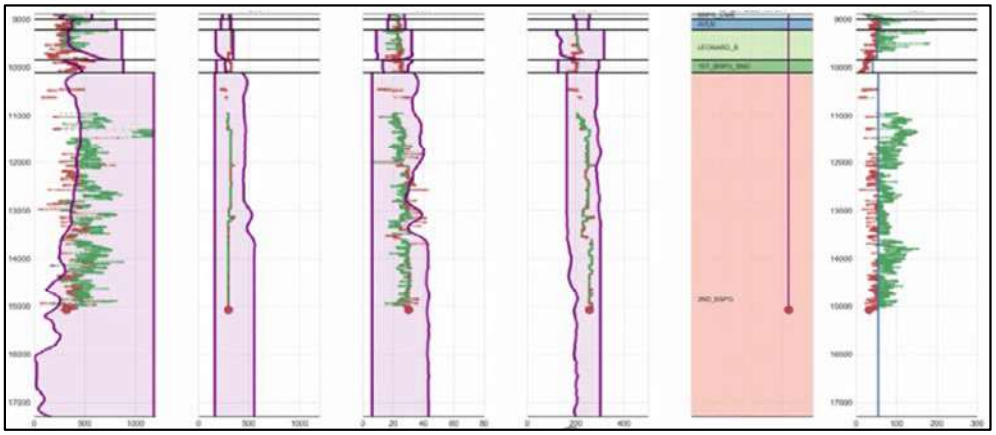

Figure 17. Testing and validation for schedule generation using data from offset wells

Conclusions

This paper introduces the concept of cloud-based ecosystem development and integration for increasing opportunities for optimization in the upstream value chain. Five main components were presented: production forecast for type wells, drilling optimization, completion design optimization, petroleum economics, and real-time AI-enhanced, or assisted, decision-making. The philosophy behind this approach is to integrate all the disciplines involved in the upstream oil & gas business and get them to look at the same data from different perspectives, with the unique goal to get the most out of a certain asset. Given the broad aspect of the proposed cloud-based solution, we decided to focus this paper on AI applications for accurate physics-based production forecasting and drilling optimization.

Two potential application for AI were discussed. Firstly, we introduced the notion of reservoir characterization via offset production data analysis to determine the key drivers of production in the formation and further characterize static reservoir and completion properties. The goal of this part of the study was to utilize physics-based reservoir models, improved with AI algorithms, to forecast production from the target reservoir accurately. Unlike typical DCA methods, that could be considered inappropriate for unconventional reservoir studies, we demonstrated that a poor understanding of the impact of physical quantities, such as static reservoir and completion properties, on well performance can result in up to 40% overestimation of EUR which, at the same time, would deliver over optimistic reservoir economics expectations.

Second, we examine the utilization of AI methods for drilling optimization, more specifically ROP optimization. We introduced several data analytics techniques, such as data filtering and data quality check, along with an ANN for ROP classification based on threshold values. We observed that, amongst the full set of parameters influencing ROP in offset wells, there were 7 parameters that had the most influence in the resulting ROP. From this finding, we constructed different modalities for ROP optimization, including 1-D, 2-D and 3-D approaches. In fact, we went as far as using the 7 parameters in the multi-dimensional space to determine the multi-dimensional groups where ROP is the optimum. However, we observed that in despite our AI model delivered accuracies as high as 90%, the accuracy dropped when we tested our model with other offset wells not previously used in the training process, i.e. test data. Nonetheless, the accuracy levels stayed around 80%, such that ROP would lie within its optimum multi-dimensional space should drilling personnel follow the recommendations of the AI algorithm to adjust one or various parameters, as required.

The other applications proposed in this study, i.e. completions optimization, petroleum economics, and AI-assisted decision-making processes, are still work in progress. The reader should be aware that the adoption of cutting-edge technologies and modern methodologies, as the one discussed in this paper, by the oil and gas industry can be slow and depends on the level of adoption E&P companies are willing to let in. Yet, we expect that given the current oil and gas markets as well as the global situation due to the COVID-19 pandemic will accelerate the adoption process henceforth opening more opportunities for field testing AI applications in the upstream value chain.

At the end of this work, we highlight that integration of domains in the upstream value chain is essential for operational efficiency and cost optimization. The integration also drives a holistic production enhancement by proactively making production-driven decisions during drilling and completions. Likewise, automated drilling and completions operations are achieved in real time by incorporating tailor made AI training models into the operations and with the goal to achieve KPI's define by the production data analysis model given by type-well analyses.

Ultimate return of investment efficiency is achieved not only by the reduction of operation cost during the drilling and completions operations. A proper production data analysis to optimize production in the target formation to achieve higher return on investment by implementing a production-driven execution of other processes, like drilling focused on production 'sweet spots' while staying in zone, engineered completions designed in real time, and petroleum economics forecasting from type-well studies.

References

Abass, H., Sierra, L., & Tahini, A. (2009). Optimizing Proppant Conductivity and Number of Hydraulic Fractures in Tight Gas Sand Wells. In *SPE Saudi Arabia Section Technical Symposium*. Society of Petroleum Engineers.

Belyadi, H., Yuyi, S., & Junca-Laplace, J. P. (2015, October). Production analysis using rate transient analysis. In *SPE Eastern Regional Meeting*. Society of Petroleum Engineers.

Brown, M., Ozkan, E., Raghavan, R., & Kazemi, H. (2011). Practical solutions for pressure-transient responses of fractured horizontal wells in unconventional shale reservoirs. *SPE Reservoir Evaluation & Engineering*, 14(06), 663-676.

Chaudhary, A. S., Ehlig-Economides, C. A., & Wattenbarger, R. A. (2011). Shale Oil Production Performance from a Stimulated Reservoir Volume. In *SPE Annual Technical Conference and Exhibition*. Society of Petroleum Engineers.

Cunningham, N. (2020). Is EIA Data Disguising A Disastrous Decline in U.S. Shale? *Oilprice.com*. Retrieved from: https://oilprice.com/Energy/Crude-Oil/Is-EIA-Data-Disguising-A-Disastrous-Decline-In-US-Shale.html

Dake, L. P. (1983). *Fundamentals of reservoir engineering*. Elsevier.

Dickson, D. (2019). Deciphering the performance puzzles in shales. *Deloitte Insights*. Deloitte Touche Tohmatsu, Ltd. Retrieved from https://www2.deloitte.com/us/en/insights/industry/oil-and-gas/us-shale-revolution-playbook/introduction-shale-performance-productivity.html

EIA, U. (2014). Updates to the EIA Eagle Ford Play Maps. US Energy Information Administration. *US Department of Energy*. Washington, District of Columbia, December.

Elliott, R. (2019). Shale Slowdown Takes Economic Toll. *The Wall Street Journal*. Dow Jones & Company. Retrieved from: https://www.wsj.com/articles/shale-slowdown-takes-economic-toll-11576405800

Fuentes-Cruz, G., & Valko, P. P. (2015). Revisiting the Dual-Porosity/Dual-Permeability Modeling of Unconventional Reservoirs: The Induced-Interporosity Flow Field. *SPE Journal*, *20*(01), 124-141.

Gherabati, S. A., Browning, J., Male, F., Ikonnikova, S. A., & McDaid, G. (2016). The impact of pressure and fluid property variation on well performance of liquid-rich Eagle Ford shale. *Journal of Natural Gas Science and Engineering*, 33, 1056-1068.

Gong, Xinglai (2013). Assessment of Eagle Ford Shale Oil and Gas Resources. *Doctoral dissertation, Texas A&M University*. Available electronically from http://hdl.handle.net/1969.1/151324.

Hughes, J. A reality check on the shale revolution. *Nature* 494**,** 307–308 (2013). https://doi.org/10.1038/494307a

Lu, H., Guo, L., Azimi, M., & Huang, K. (2019). Oil and Gas 4.0 era: A systematic review and outlook. *Computers in Industry*, *111*, 68-90.

Mayerhofer, M. J., Lolon, E., Warpinski, N. R., Cipolla, C. L., Walser, D. W., & Rightmire, C. M. (2010). What is Stimulated Reservoir Volume?. *SPE Production & Operations*, 25(01), 89-98.

McCain Jr, W. D. (2017). Properties of Petroleum Fluids. Third edition. PennWell Corporation.

Molina, O. M., "Application of Pressure and Rate Transient Analyses to Stress-Sensitive Multi-Fractured Composite Systems and Compartmentalized Reservoirs" (2019). *LSU Doctoral Dissertations*. 4938.

Oliver, D. S., Reynolds, A. C., & Liu, N. (2008). *Inverse theory for petroleum reservoir characterization and history matching*.

Ozili, P. K. and Arun, T. (2020). Spillover of COVID-19: Impact on the Global Economy. Available at SSRN: https://ssrn.com/abstract=3562570 or http://dx.doi.org/10.2139/ssrn.3562570

Stalgorova, K., & Mattar, L. (2013). Analytical Model for Unconventional Multifractured Composite Systems. *SPE Reservoir Evaluation & Engineering*, 16(03), 246-256.

Smith, M. B., & Montgomery, C. (2015). Hydraulic Fracturing. CRC Press.

Spivey, J. P., & Lee, W. J. (2013). *Applied Well Test Interpretation* (pp. 1-30). Richardson, TX: Society of Petroleum Engineers.

Sureshjani, M. H., Ahmadi, M., & Fahimpour, J. (2020). Uncertainty Quantification in Heterogeneous Tight/shale Reservoirs from Analysis of Transient/Boundary-Dominated Production Data. *Journal of Natural Gas Science and Engineering*, 103342.

Wang, H. 2017. What Factors Control Shale Gas Production and Production Decline Trend in Fractured Systems: A Comprehensive Analysis and Investigation. *SPE Journal*, 22(02): 562-581. http://dx.doi.org/10.2118/179967-PA

Yao, S., Zeng, F. & Liu, H. A semi-analytical model for hydraulically fractured horizontal wells with stress-sensitive conductivities. *Environ Earth Sci* 75, 34 (2016).

Yusuf, Ahmed, "Integrating stimulation practices with geo-mechanical properties in liquid-rich plays of Eagle Ford Shale" (2016). *Graduate Theses, Dissertations, and Problem Reports*. 7019.

Zhang, J., Kamenov, A., Hill, A. D., & Zhu, D. (2014). Laboratory Measurement of Hydraulic-Fracture Conductivities in the Barnett Shale. *SPE Production & Operations*, 29(03), 216-227.